Phi: Jurnal Pendidikan Fisika dan Terapan
Vol. 12, No. 2 (2026) 231-238
ISSN: 2460-4348, e-ISSN: 2549-7162
https://jurnal.ar-raniry.ac.id/index.php/jurnalphi/index

Article Type: *original research*

Identification of Subsurface Structures in Jaboi Hot Spring Sabang Using Electrical Resistivity Tomography

Dian Darisma[1*], Syafrizal Idris[2], Badrul Munir[1], Marwan Marwan[1], Rifa Salma Salsabila[1]
[1]Department of Geophysical Engineering, University of Syiah Kuala, Banda Aceh, Indonesia
[2]Department of Physics Education, University of Malikussaleh, Banda Aceh, Indonesia

Correspondence E-mail: diandarisma@usk.ac.id

ARTICLE INFO

Article History:
Received: 23 January 2026
Revised: 30 April 2026
Accepted: 24 May 2026
Published: 08 June 2026

Keywords:
Resistivity; Jaboi; Geothermal; Hot Spring; Tomography

ABSTRACT

The Jaboi geothermal field possesses a capacity of 50 MWe and is set to be developed into a power plant with a configuration of 2x5 MWe. This study seeks to develop a more detailed subsurface model utilizing the two-dimensional electrical resistivity tomography near Jaboi hot spring. This study employs the Wenner-Sclumberger configuration, which effectively characterizes subsurface models in horizontal and vertical dimensions. This method effectively models subsurface conditions by categorizing the resistivity values of rocks into three distinct layers. From line JB1, it can be interpreted as a fluid path, supported by the presence of surface manifestations. It remains uncertain whether a fluid path is present in line JB2. The rock interpretation results at the study site indicate a predominance of tuff mixed with pumice flakes and sandstone and clay tuff combined with agglomerates. The aquifer layer at the study site begins at a depth of 50 m, exhibiting a resistivity value ranging from 2 to 10 Ωm.

This work is licensed under a Creative Commons Attribution-ShareAlike 4.0 International License

1. INTRODUCTION

1.1 Background and Objectives

Indonesia has significant geothermal energy potential across 331 sites, with resources amounting to 11,073 MW and reserves totaling 17,506 MW (EBTKE and ESDM, 2017). Aceh shares significant geothermal potential in Indonesia, totaling 1310 MW across 17 sites. Among these locations, Jaboi exhibits geothermal potential that is suitable for establishing a geothermal power plant. Jaboi is a geothermal field with an estimated capacity of 50 MWe and an initial development plan of 2x5 MWe (EBTKE and ESDM, 2017).

The Jaboi geothermal system lies along a volcanic arc, a favorable geological setting for geothermal activity due to heat sources, fractured reservoirs, and convective groundwater systems (Dwipa et al., 2006). Surface manifestations such as hot springs have been identified on Weh Island, particularly in the vicinity of Jaboi, indicating the presence of active geothermal processes (Figure 1). These manifestations are typically associated with structural features like local faults and fracture zones, which serve as conduits for fluid flow. Previous studies have shown that such structures can be effectively delineated using geophysical techniques such as gravity surveys (Basantaray and Mandal,

2022; Omollo and Nishijima, 2023) and electrical resistivity tomography (Darisma et al., 2020; Singh et al., 2021).

Earlier investigations in the Jaboi area employed the Vertical Electrical Sounding (VES) method to assess the subsurface resistivity around the Jaboi volcano and the Ceunohot (Marwan et al., 2019; Yanis et al., 2024). While useful for one-dimensional subsurface interpretation, the VES method provides limited resolution of complex geological features (Kumar et al., 2007), which often fail to resolve lateral heterogeneities and the steeply dipping structure common in volcanic tectonic environments like Jaboi. This study applied the two-dimensional electrical resistivity tomography, which provides improved spatial resolution and enables a thorough investigation of lateral and vertical resistive changes for describing subsurface conditions (Idris et al., 2022; Nguyen et al., 2005; Loke et al., 2013). Parameter resistivity is one useful geophysical parameter to predict and identify the position and geometry of small geological structures, which usually control the occurrence of geothermal manifestations.

Essential for understanding the geothermal system in the Jaboi hot spring area, this work attempts to define and characterize subsurface formations, including faults, fractures, aquifers, and lithological interfaces, and ERT offers superior geometric fidelity in mapping vertical fluid conduits (Arango-galvan et al., 2016). ERT methods have been proven effective in delineating both shallow and deep aquifer systems based on resistivity contrasts (Darsono, 2016). Two-dimensional electrical resistivity tomographys would help estimate geothermal potential and support upcoming local exploration and development projects.

1.2 Geological Setting

The segmentation of the Sumatran Fault Zone in the Aceh region, particularly the Seulimum and Aceh segments, significantly influences the distribution of permeability and hydrothermal upflow zones in local volcanic fields (Bennet, 1981). The geological structure of Weh Island exhibits a pattern analogous to that of the Sumatran Fault. The fault zone on Weh Island exhibits continuity with the Seulimum fault, associated with the Seulawah Agam volcano, which intersects the Krueng Raya bay on the mainland of Aceh (Sieh & Natawidjaja, 2000). Fault zones on Weh Island predominantly exhibit a NW-SE orientation, as evidenced in Balohan Bay, extending towards Sabang Bay. The Ujung Seuke and Balohan faults create a graben characterized by cliffs to the east of Balohan Bay. Lake Aneuk Laot, located in the southern region of Sabang, is anticipated to form due to subsidence rather than from the volcanic eruption center. The Paya Seunara Fault is located to the west of the graben structure, while the Jaboi Fault, oriented in a north-south direction, is situated to the south.

Weh Island is classified as a type C volcano, representing an unidentified eruption center that exhibits characteristics of a fumarole field based on its historical activity (De Neve, 1983). Dirasutisna and Hasan (2005)characterize the lithology of Weh Island, which consists of Tertiary and Quaternary rocks categorized into four primary groups: one is the Tertiary (Miocene) sedimentary rock group this basement unit comprises the tuffaceous sandstone (Tms) and reef limestone (Qqt), the Tms formation act as a relatively impermeable unit unless fractured, second is the older volcanic rock group from Weh Island of Quaternary-Tertiary age composed of lava and pyroclastic flows this group includes the iboih volcanic (Qvl) and pulau weh phyroclastic flow (Qtapw), these units consist of densified andesitic lava and breccias which may serve as the heat conductor from deeper sources, third is the Quaternary young volcanic rock group comprising a series of young volcanic cones arranged in northwest-southeast and north-south orientations, and a group of limestone reefs.

Weh Island features several primary faults (Figure 1), predominantly normal faults, which are the geological structures that underlie the geothermal system. Secondary faults have also developed in this area due to tectonic processes, including the Leumoo Matee fault (LM), Ceunohot fault (CT), and Jaboi fault (JB) form a structural network that directs the upflow of hydrothermal fluids. The Jaboi fault, oriented North-South, is specifically associated with the surface manifestations analyzed in this study. The interaction of these faults creates high vertical permeability zones, which are essential for the convection of the geothermal system.

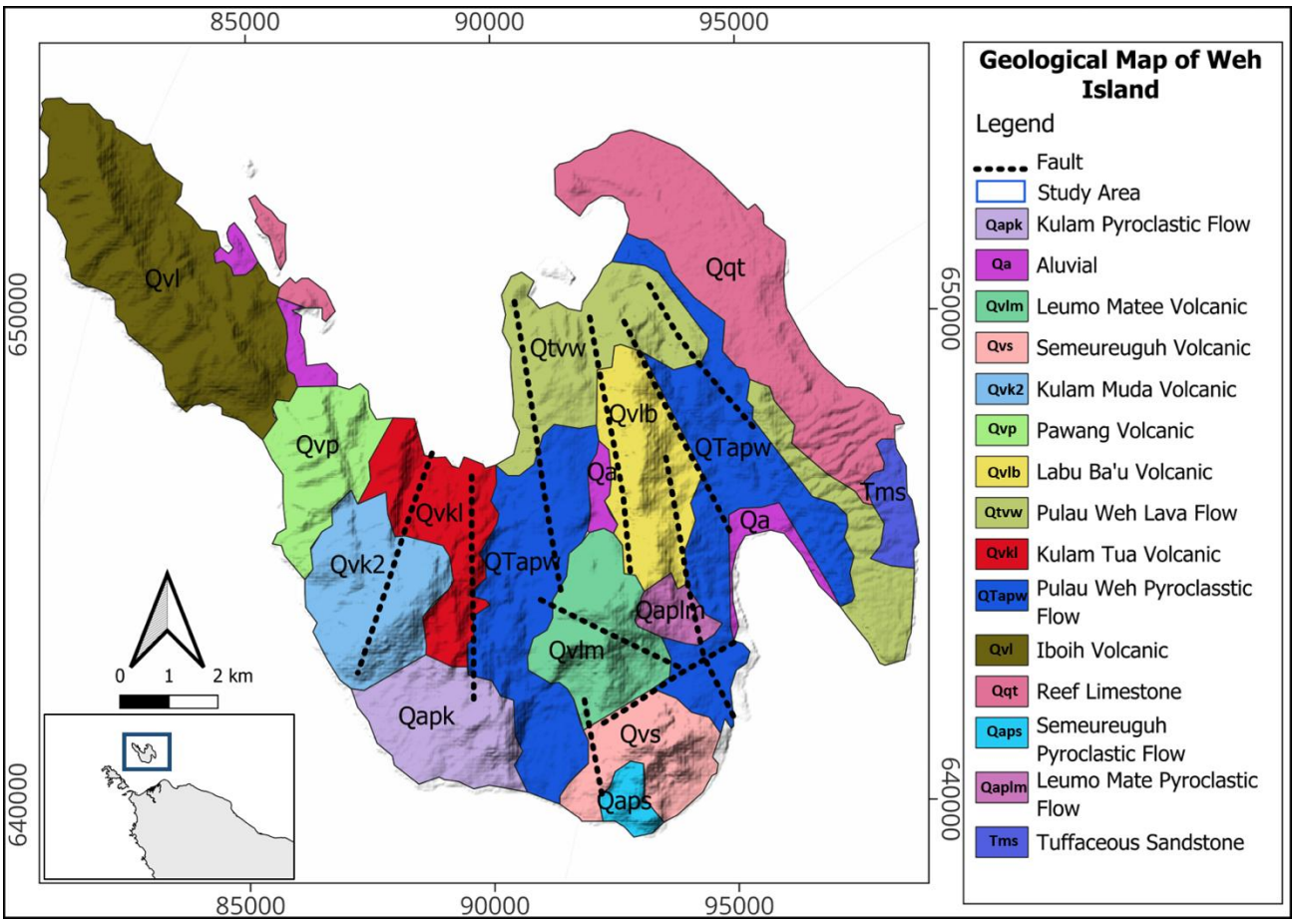


Figure 1. Weh Island's geological map (modified from Dirasutisna and Hasan, 2005)

2. METHODS

The electrical resistivity tomography is a geophysical technique employed to ascertain the physical properties of underground rocks by analyzing rock resistivity (Reynolds, 2011). The rock's resistivity value indicates the subsurface formations' physical state. This approach yields the perceived resistivity (ρa) rather than the true resistivity, shown by

$$\rho_a = K \frac{\Delta V}{I} \tag{1}$$

K represents the geometric factor, ΔV denotes the potential difference, and I signifies the current. The Earth consists of distinct layers, each exhibiting varying resistivity values.

The guidelines for electrode placement in the geoelectrical approach are referred to as electrode configurations. The employed configuration results in a distinct geometry factor for each arrangement. The geometry factor quantifies the adjustment of the arrangement of both the potential and current electrodes. This study used the Wenner-Schlumberger setup (Figure 2).

The Wenner-Schlumberger design integrates the Wenner and Schlumberger configurations (Dahlin, 2001). In this arrangement, the separation between electrodes P1 and P2 is denoted as a, whereas the distance between C1P1 and P2C2 is represented as na. The inter-electrode spacing is fixed, providing excellent horizontal coverage and effective depth penetration. The combination of Wenner and Schlumberger leads to a modification of the k value of the geometric factors, specifically:

$$k = \pi n(n+1)a \tag{2}$$

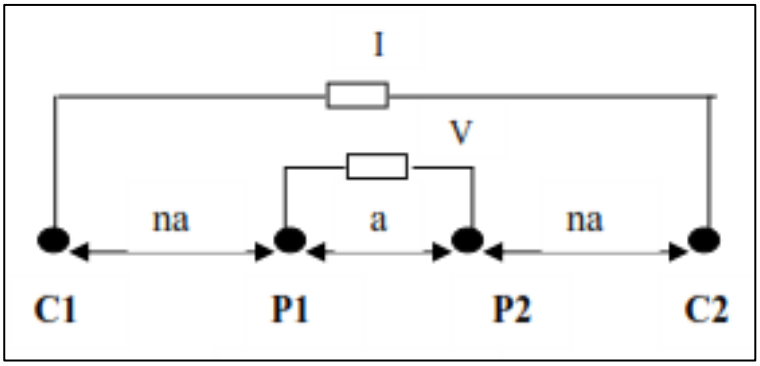


Figure 2. Setting of current and potential electrodes for electrical resistivity measurement (Telford et al., 1990).

This study was conducted on the Jaboi coast in Sabang. The measurement line comprises two segments, JB1 and JB2, with the JB1 path near the hot spring manifestation (Figure 3). Data acquisition using a design survey with two lines of 395 m in length, with an inter-electrode spacing of 6 m, with height and positional data recorded at each electrode by GPS. The selection of a 6 m electrode spacing ensures sufficient depth penetration while maintaining the spatial resolution necessary to detect the local fracture zone associated with hydrothermal upflow (Kneisel et al., 2006). This research employed RES2DINV (Loke, 2002) for data processing, using the least-squares optimization method to determine subsurface geological conditions. This application generates inverse pseudosections of resistivity, defines windows, and presents a two-dimensional subsurface resistivity model derived from survey data.

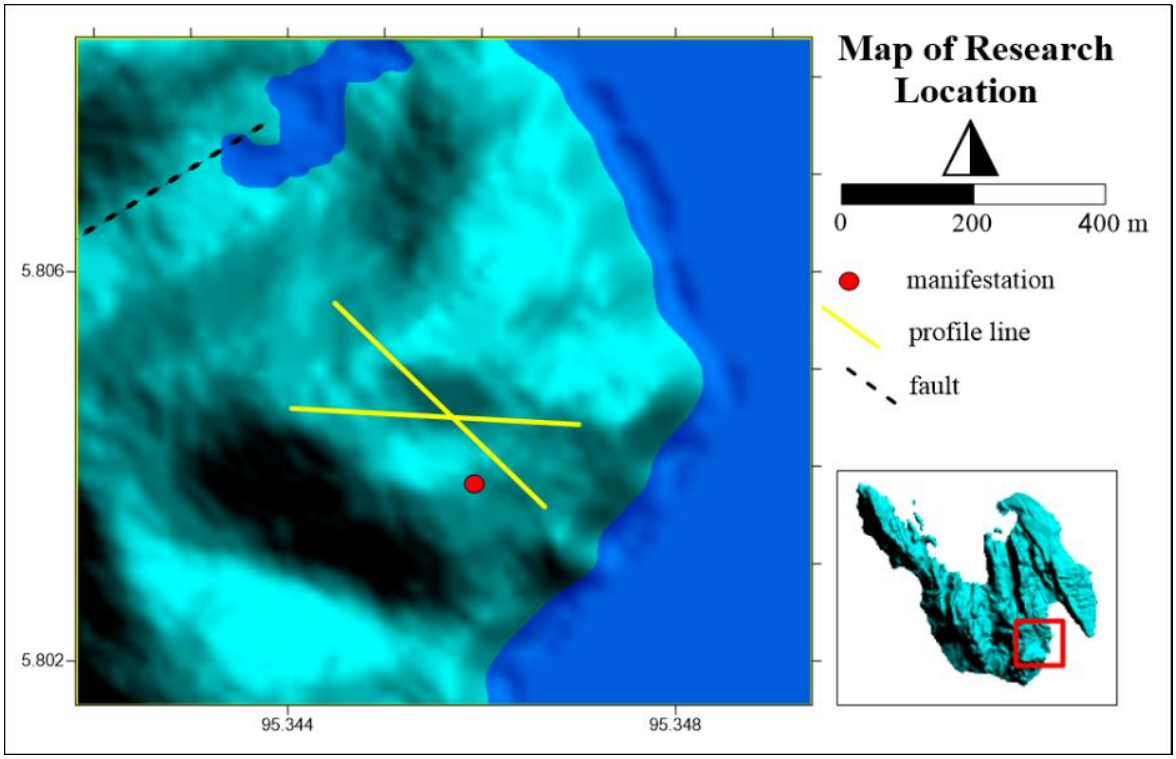


Figure 3. The research location map of two measurement lines, JB1 and JB2, near the hot spring manifestation

3. RESULT AND DISCUSSION

Multiple factors, such as porosity, permeability, and fluid types, can affect the resistivity of rock. The porosity and permeability of the rock create voids that can be occupied by fluid, resulting in diminished rock resistivity. The resistivity model for line JB1 is interpreted as possessing a fluid conduit to the surface, confirmed by surface manifestations (Figure 4). In geothermal environments, increased porosity and the presence of mineralized hydrothermal fluids typically reduce resistivity. The 2D inversion results for line JB1 and JB2 (Figure 4 and 5) show a wide resistivity range from <2 Ωm to > 200 Ωm, reflecting the complex interaction between volcanic products and geothermal fluids.

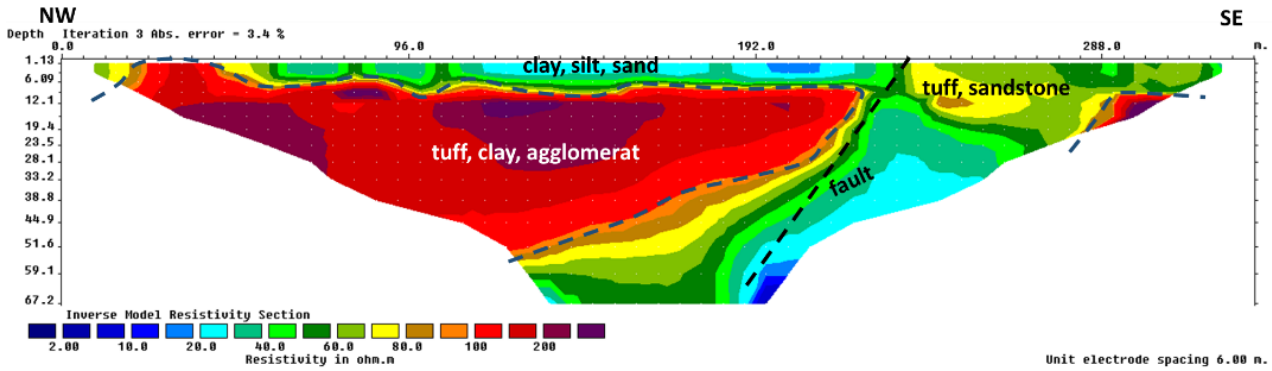


Figure 4. Results of two-dimensional resistivity inversion at line JB 1 with rock interpretation

The resistivity model was coupled with drilling data (Munandar et al., 2006). The uppermost layer for line JB1 is characterized as a mixture of clay, silt, and sand, ranging from fine to coarse, interspersed with pumice stone, extending to a depth of 12 meters, exhibiting a resistivity value of 10-50 Ωm. The volcanic region's geological features facilitate the production of a pumice stone mixture inside the rock strata. Nevertheless, because of the substantial measuring interval of 6 m, the pumice stones, which are scarce among the other rocks, are absent.

The layer located at a distance range 0-230 m, extending depth from 12 to 51 m, with a resistivity of 100-300 Ωm, is primarily composed of clay interspersed with agglomerates, rendering this layer impermeable to water. This layer also contains plentiful pumice stone and andesite fragments. A resistivity value of 50-100 Ωm is recorded at a distance of 230-330 m. The rock comprises a predominant tuff, with a layer of pumice above and a strong sandstone interspersed with tuff and pumice beneath. The JB1 line reveals an aquifer layer characterized by low resistivity values (conductive) of less than 10 Ωm, located at a depth of 59 m and extending to a distance of 190 m. This aquifer layer consists of sandstone characterized by high porosity.

A critical feature in JB1 is the subvertical conductive anomaly <10 Ωm identified at depth approximately 59 m. This zone is interprets as a fault controlled fluid conduit. The structural geometry, specifically the identified fault plane (as marked in Figure 4), creates a vertical pathway (upflow zone) that allows geothermal fluids to migrate toward the surface, feeding the observed manifestations in Jaboi. The high porosity of the sandstone aquifer at this depth likely facilitates significant fluid storage and transport.

A layer including clay, silt, and sand with fine roughness intermixed with pumice is located along line JB2 (Figure 5) at a distance of 120-198 m at a depth of 0-12 m exhibiting a resistivity value of 10-50 Ωm. The predominant layer of clay interspersed with agglomerates was identified at a range of 108-230 m at a depth of 12-51 m with high resistivity layer >100 Ωm.JB2It is also characterized as rocks primarily composed of tuff interspersed with pumice fragments at the surface, and sandstone combined with tuff and pumice fragments in the deeper layers exhibiting a resistivity value of 50-100 Ωm. At a depth of 51-55 meters, a dense silt sand is present, transitioning to a layer of sand that extends constantly eastward from a distance of 55 meters to 236 meters exhibiting a resistivity value of 10-50 Ωm.

The JB2 line also reveals an aquifer layer characterized by low resistivity values (conductive) of less than 10 Ωm, located at a depth of 56 m and extending to a distance of 120-198 m. This aquifer layer consists of sandstone characterized by high porosity and indicative of intensive hydrothermal alteration, where primary volcanic minerals are transformed into conductive clay minerals such as smectite (Revil et al., 2010).

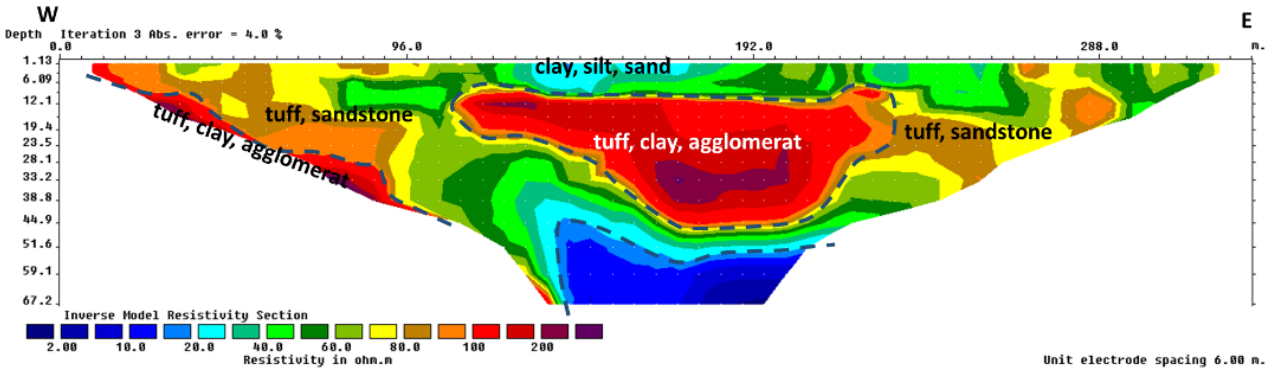


Figure 5. Results of two-dimensional resistivity inversion at line JB 2 with rock interpretation

4. CONCLUSION

This research characterized the subsurface structural framework of the geothermal Jaboi using ERT and integration with geological information lead to several key conclusions:

1. Identification of hydrothermal conduits, a significant subvertical conductive anomaly <10 Ωm was identified in Line JB1, which is interpreted as a primary fault that controlled fluid pathway. This structure serves as the main upflow zone.
2. Identification geothermal system in the study area is a resistive layer (100-300 Ωm) composed of volcanic agglomerates acts as an impermeable seal, overlying a conductive reservoir zone (2-10 Ωm), identified in Line JB2.
3. The resistivity values in the research area range from 10 to 50 Ωm, corresponding to clay, silt, and sand strata. A resistivity value of 50-100 Ωm indicates a layer of tuff interspersed with pumice fragments and sandstone. The resistivity range of 100-300 Ωm is regarded as a combination of clay tuff and agglomerates. The rock interpretation results at the research site indicate a predominance of tuff interspersed with pumice fragments and sandstone and clay tuff combined with agglomerates.

ACKNOWLEDGEMENTS

We want to thank all students from the Geophysical Engineering Department of the University of Syiah Kuala who are involved in data acquisition.

REFERENCES

Arango-Galván, C., Prol-Ledesma, R. M., Flores-Márquez, E. L., & Banda-Hernández, J. (2016). The use of electrical resistivity tomography (ERT) for the characterization of a geothermal field. *Journal of Applied Geophysics*, 128, 137-145.https://doi.org/10.22201/igeof.00l67169p.2022.61.4.2228.

Basantaray, A.K., Mandal, A. (2022). Interpretation of gravity–magnetic anomalies to delineate subsurface configuration beneath east geothermal province along the Mahanadi rift basin: a case study of non-volcanic hot springs. *Geothermal Energy* 10, 6.https://doi.org/10.1186/s40517-022-00216-4

Bennet, J. D. (1981). *Peta Geologi Lembar Banda Aceh*. Pusat Penelitian dan Pengembangan Geologi.

Dahlin, T. (2001). The development of DC resistivity imaging techniques. *Computers & Geosciences* 27, 1019–1029.https://doi.org/10.1016/S0098-3004(00)00160-6

Darisma, D., Fernanda, F., Syukri, M. (2020). Investigation of Groundwater Potential using Electrical Resistivity Method and Hydraulic Parameters in Lam Apeng, Aceh Besar, Indonesia. *Journal of Geoscience, Engineering, Environment, and Technology* 5, 185–190. https://doi.org/10.25299/jgeet.2020.5.4.5501

Darsono (2016). Identifikasi Akuifer Dangkal dan Akuifer Dalam dengan Metode Geolistrik (Kasus: Di Kecamatan Masaran). *Indonesian Journal of Applied Physics*, 6(1), 40-49.https://doi.org/10.13057/ijap.v6i01.1798

De Neve, G. (1983). *Quaternary Volcanism and Other Phenomena Attribute to Volcanocity in the Aceh Region North Sumatra*. Proceedings PIT XII Ikatan Ahli Geologi Indonesia 67–90.

Dirasutisna, S., Hasan, A.R., 2005. *Geologi Panas Bumi Jaboi, Sabang, Propinsi Aceh Nangroe Darussalam*. Direktorat Inventarisasi Sumber Daya Mineral, Bandung.

Dwipa, S., Widodo, S., Suhanto, E., Kusnadi, D. (2006). *INTEGRATED GEOLOGICAL, GEOCHEMICAL AND GEOPHYSICAL SURVEY IN JABOI GEOTHERMAL FIELD, NANGRO ACEH DARUSSALAM, INDONESIA*. Proceedings of the 7th Asian Geothermal Symposium .https://www.geothermalenergy.org/pdf/IGAstandard/Asian/2006/20_dwipa.pdf.

EBTKE, D., ESDM, B.G.K. (2017). *Buku Potensi Panas Bumi Jilid 1*. Jl. Pegangsaan Timur.

Idris, S., Darisma, D., Pramana, A.H., Aflah, N., Sayuti, M., Novita, N. (2022). Identification of the Aquifer Layer using the Geoelectric Method in Teupin Batee Village, Aceh Besar. *Bulletin of Computer Science and Electrical Engineering* 3, 40–46. https://doi.org/10.25008/bcsee.v3i1.1155

Kumar, D., Ahmed, S., Krishnamurthy, N., Dewandel, B. (2007). Reducing ambiguities in vertical electrical sounding interpretations: A geostatistical application. *Journal of Applied Geophysics* 62, 16–32. https://doi.org/10.1016/j.jappgeo.2006.07.001

Kneisel, C., Rödder, T., Roth, N., & Schwindt, D. (2014). Electrical resistivity monitoring for the detection of changes in mountain permafrost at different time scales. *Permafrost and Periglaciation Processes*, 25(2), 105-119.

Loke, M. (2002). *Rapid 2-D Resistivity and IP inversion using the least-squares method, Geoelectrical Imaging 2D and 3D*. Geotomo Softw.

Loke, M. H., Chambers, J. E., Rucker, D. F., Kuras, O., & Wilkison, P.B. (2013). Recent developments in the direct-current geoelectrical imaging method. *Journal of Applied Geophysics*, 95, 135-156. https://doi.org/10.1016/j.jappgeo.2013.02.017

Marwan, M., Rifqan, R., Syafrizal, I., Muhammad, Y. (2019). Application of vertical electrical sounding (VES) for subsurface profiling in Weh Island, Aceh Province. *Aceh International Journal of Science and Technology* 8, 29–34. https://doi.org/10.13170/aijst.8.1.12879

Munandar, A., Boegis, Z., Simarmata, R.S. (2006). *PEMBORAN LANDAIAN SUHU SUMUR JBO-1 DAN JBO-2 DAERAH PANAS BUMI JABOI, P. WEH, KOTA SABANG–NAD*. Proceeding Pemaparan Hasil-hasil

Kegiatan Lapangan dan Non-Lapangan Tahun 2006, Pusat Sumber Daya Geologi

Nguyen, F., Garambois, S., Jongmans, D., Pirard, E., Loke, M. (2005). Image processing of 2D resistivity data for imaging faults. *Journal of Applied Geophysics* 57, 260–277. https://doi.org/10.1016/j.jappgeo.2005.02.001

Omollo, P., Nishijima, J. (2023). Analysis and interpretation of the gravity data to delineate subsurface structural geometry of the Olkaria geothermal reservoir, Kenya. *Geothermics* 110, 102663. https://doi.org/10.1016/j.geothermics.2023.102663

Reynolds, J.M. (2011). *An introduction to applied and environmental geophysics*. John Wiley & Sons.

Revil, A., et al. (2010). The hydrothermal system volcan de Colima (Mexico) inferred from selfpotential, electrical resistivity, and temperature measurements. *Journal of Volcanology and Geothermal Research*, 192(1-2), 19-35. https://doi.org/10.22201/igeof.00167169p.1986.25.4.779

Sieh, K., Natawidjaja, D. (2000). Neotectonics of the Sumatran fault, Indonesia. *Journal of Geophysical Research: Solid Earth* 105, 28295–28326. https://doi.org/10.1029/2000JB900120

Singh, Somvir, Gautam, P.K., Bagchi, D., Singh, Sashikant, Kumar, S., Kannaujiya, S. (2021). 2D electrical resistivity imaging for geothermal groundwater characterization and rejuvenation of the Gaurikund hot spring in the Main Central Thrust (MCT) zone of the Garhwal Himalaya, Uttrakhand, India. *Groundwater for Sustainable Development* 15, 100686. https://doi.org/10.1016/j.gsd.2021.100686

Telford, W.M., Geldart, L.P., Sheriff, R.E. (1990). *Applied geophysics*. Cambridge university press.

Yanis, M., Zaini, N., Abdullah, F., Isa, M., Marwan, M., Idris, S., Paembonan, A.Y., Ananda, R., Zainal, M., Ghani, A.A., Saputra, D. (2024). Vertical electrical sounding for revealing the groundwater resources in the geothermal spring of Jaboi volcano. *Acta Geophys*. 72, 1617–1635. https://doi.org/10.1007/s11600-023-01164-8